

## Research Article

# Optimization of the Process Parameters for the Preparation of Activated Carbon from Low Cost Phoenix Dactylifera Using Response Surface Methodology

**Devi AS, Kalavathy MH and Miranda LR\***  
Carbon Research and Engineering, Department of Chemical Engineering, A.C. Tech, Anna University, Chennai, India

**\*Corresponding author:** Lima Rose Miranda, Carbon Research and Engineering, Department of Chemical Engineering, A.C. Tech, Anna University, Chennai, India

**Received:** November 23, 2015; **Accepted:** December 30, 2015; **Published:** December 31, 2015

**Abstract**

This work deals with the preparation of low-cost activated carbon from selected agricultural waste materials, by chemical activation with orthophosphoric acid. Activated carbon was prepared at various temperature, time and impregnation ratio. The effect of these preparation parameters on the yield and adsorption capacity of the prepared activated carbon was analyzed. The activation process was confirmed by the well-developed pore structure seen in SEM image and the FTIR analysis. The significant effect of three important process parameters were investigated systematically and optimized preparation condition was determined for the prepared ACDP to separate out different dyes of varying molecular weight range using Response Surface Methodology. This work showed that the effectiveness of an adsorbent lies in the way it is prepared and tuning the preparation condition directly has effect on the pore structure. The results reveal that ACDP can be recommended as a potential adsorbent for effective removal of pollutants from waste water and aqueous solutions.

**Keywords:** Activated carbon; Chemical activation; Characterization; Optimization; Response Surface Methodology

**Abbreviations**

AC	Activated Carbon
ACDP	Activated Carbon from date pits
CCD	Central Composite Design
FTIR	Fourier Transform Infrared Spectroscopy
IN	Iodine Number
MB	Methylene Blue
MR	Methyl Red
MG	Malachite green
MV	Methyl Violet
MBN	Methylene Blue Number
MRN	Methyl Red Number
MGN	Malachite green Number
MVN	Methyl Violet Number
RSM	Response Surface Methodology
SEM	Scanning Electron microscope
TGA	Thermo gravimetric analysis

**Introduction**

Among the various technologies available to remove toxic components such as anions, heavy metals, organic compounds and dyes from water sources, adsorption has been shown to be very

effective for removal of dyes and other pollutants from aqueous solutions [1]. Activated carbon-based systems can remove a wide variety of toxic pollutants with very high removal efficiencies and has proved to be the least expensive treatment option, particularly in treating low concentrations of wastewater streams and in meeting stringent treatment levels. (Figure 1) shows the surface attraction of gases and chemicals onto activated carbon. This widely used adsorbent in industrial scale is commercially manufactured from various carbonaceous precursors like lignite and coal (42%), peat (10%), wood (33%) and coconut shell. However, the growing demand in adsorbing materials for polluted fluids treatment and increased cost of raw materials resulted in an increased research, concerning activated carbon preparation methods and sources.

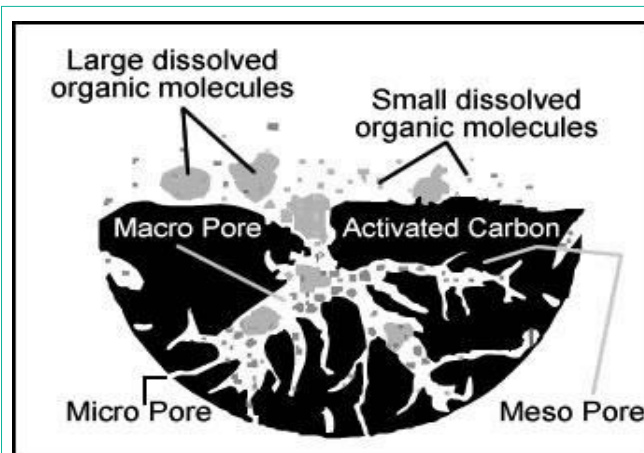


**Figure 1:** Structure of activated carbon.



Figure 2: Raw date pits.

In recent years, researchers have used low cost materials and waste agricultural material to reduce the cost of production. These include palm ash [2,3], chitosan/oil palm ash composite beads [4], pomelo (*Citrus grandis*) peel [5], salts treated beech sawdust [6], waste materials [7], natural *Luffa cylindrica* fibres [8], sunflower seed shells [9], algal biomass based materials [10], wheat bran [11], guava (*Psidium guajava*) leaf powder [12], almond shells [13], dehydrated peanut hull [14], rubber wood sawdust [15], *Moringa oleifera* wood [16], *Agave sisalana* fibre [17] and wheat shells [18]. But however, adsorption capacity and regeneration capacity for further cycle is limited. Thus, subverting the above mentioned disadvantages, porous activated carbon prepared from date pits (*Phoenix dactylifera* (Figure 2) by phosphoric acid activation method is being adopted in this study. Further, efficiency of the adsorption process depends on the type of precursor we use and how it is being prepared.

This work aims at reducing the heating time and chemical usage to determine the optimum preparation conditions for effectively removing a particular pollutant of particular molecular weight from an aqueous solution. The effects of the activation temperature, activation time and the impregnation ratio on the surface and chemical properties of activated carbon are studied to determine the optimum preparation conditions. Response Surface Methodology (RSM) was used to optimize preparation parameters of AC for separately removing four such dyes: Methyl red (molecular weight – 269.30), Methylene blue (molecular weight – 319.85), Malachite green (molecular weight – 36.91), Methyl violet (molecular weight – 407.98) and molecules less than 2 nm size from aqueous solution.

## Materials and Methods

### Materials

The Date pits were collected in bulk from small scale industries from a local village of virudhunagar district, Tamil Nadu. Phosphoric acid and hydrochloric acid were obtained from Ranbaxy Fine Chemicals Ltd, Chennai, India. Potassium iodide, iodine and sodium thiosulphate were procured from Sisco Research Laboratories, India.

The dyes such as Methylene blue, Malachite green, Methyl violet and Methyl red were purchased from Sigma Aldrich Chemicals, India. All the chemicals used were of analytical grade. Distilled water was used for all the experimental purposes.

### Preparation of activated carbon

The precursor was first cut into small pieces then washed with distilled water to remove undesirable impurities and dried in sunlight for 7 days and then at 80°C for 4 hours. The dried precursor was powdered and sieved through a 30 mesh sieve. The prepared precursor was then chemical activated with the use of phosphoric acid as activating agent. The precursor impregnated with 85 wt% phosphoric acid was placed in an autoclave and activated in a muffle furnace. The sample was heated in the absence of air to the activation temperature at a heating rate of 20°C/min and held at that temperature for the desired activation time. Activated carbon samples were prepared at different conditions by varying three factors namely activation time, activation temperature and the impregnation ratio. The impregnation ratio is defined as the ratio of dried weight of  $H_3PO_4$  to the dried weight of precursor. These factors are varied at three levels each. After gradual cooling down to room temperature, the final activated product was repeatedly washed with hot distilled water until the wash water reaches constant pH. The washed carbon was dried in oven at 110°C for 24 hours, and finally kept in tightly closed bottles.

### Characterisation of the Activated Carbon

**Yield:** The yield of the prepared activated carbon was calculated from the following formula,

$$\text{Yield (\%)} = W_2/W_1 * 100 \quad (1)$$

Where  $W_1$  and  $W_2$  are weights of the precursor and final activated carbon obtained respectively, both based on dry weight.

**Iodine number:** 1 g of the carbon samples were transferred to a clean, dry 250 mL Erlenmeyer flask. 10 mL of 5 wt % hydrochloric acid solution was pipetted into each flask. The flasks were closed and gently swirled until the carbon was completely wet. The contents of the flasks were allowed to boil gently for  $30 \pm 2$  s to remove any sulphur which may interfere with the results. The flasks were then removed from the hot plate and cooled to room temperature. To this, 100 mL of 0.1 N iodine solution was added and the flasks were shaken vigorously for  $30 \pm 1$  s. The contents of the flasks were filtered. 50 mL of the filtrate were taken in 250 mL Erlenmeyer flask and titrated against standardized 0.1 N sodium thiosulphate solutions until the solution turned pale yellow. 2 mL of the starch indicator was added to this solution and the titration was continued with sodium thiosulfate until the solution turned colourless. The volume of sodium thiosulphate used was recorded and the amount of iodine adsorbed per g of carbon dosage was calculated [19].

The value of iodine number can be calculated using,

$$\frac{X}{M} = \frac{(A - (DF)(B)(S))}{M} \quad (2)$$

where, X/M is iodine adsorbed per gram of activated carbon (mg/g), S is volume of sodium thiosulfate used (mL) and M is amount of activated carbon used (g).

**Table 1:** Experimental design with factors and levels.

Variables	Symbol	Coded factor levels		
		-1	0	1
Temperature	A	350	400	450
Time	B	30	60	90
Impregnation ratio	C	1	2	3

$$A = (N_1) \times 12693$$

$$B = (N_2) \times 126.93$$

$$DF = (I + H) / F$$

$N_1$  is the normality of iodine (N),  $N_2$  is the normality of sodium thiosulphate (N), DF is dilution factor, I is volume of iodine (mL), H is 5 % hydrochloric acid used (mL), and F is filtrate (mL).

**Methylene blue, malachite green, methyl violet and methyl red number:** A known weight of activated carbon was taken in four different conical flasks. 10 mL of 1500 mg/L MB dye, MG dye, MV dye and MR dye solution were added and shaken for 5 min. After the solution got decolorized, the addition of dye was continued to their respective flasks (1 mL at a time) till no further color change was observed. The decolorizing power was determined from the following equation [20].

$$\text{Decolorizing power} = (1.5 \times V_m) / M \quad (3)$$

where  $V_m$  is the volume of dye solution consumed (mL), M is the amount of carbon sample taken (g).

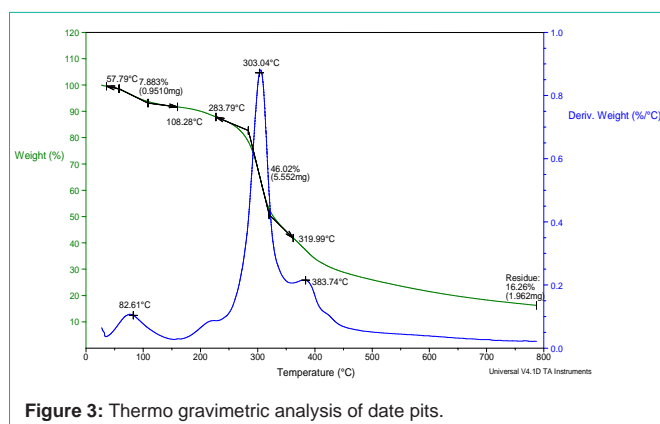
**Thermo gravimetric analysis (TGA):** In order to determine general decomposition characteristics of the biomass source during the activation, the sample was subjected to thermo gravimetric analysis (Perkin Elmer Pyris TG/DTA). The volatile evolution during carbonization of the samples was monitored by TGA.

**Scanning electron microscopy (SEM):** In order to observe the surface morphology of the adsorbent, a scanning electron microscopic analysis of raw source and the activated sample was employed in this study. SEM images were recorded using JEOL JSM-6300F field emission.

**Fourier transform infrared spectroscopy (FTIR):** The surface functional groups of samples were analyzed through FT-IR transmission spectra recorded using a FTIR spectrophotometer (FTIR-2000, Perkin-Elmer) in the wave number range of 4000-400  $\text{cm}^{-1}$ .

### Experimental design – response surface methodology

Box-Behnken design: Although many techniques are available to optimize the response of interest which is influenced by several other variables, RSM is one of the simplest and the best [21,22]. The main advantage of this method is that it gives an understanding of how the desired process response is affected by the process variables, establishes all expected interactions among the process variables and depicts the combined effect of the test variables on the response. Also, when there is more than one response, it finds the compromise optimum rather than optimizing only one. It gives an understanding of how response changes in a given direction by adjusting the design variables. From literature, it was found that no studies has been

**Figure 3:** Thermo gravimetric analysis of date pits.

conducted and reported for preparation of activated carbon from date pits by chemical activation adopting RSM as the optimization tool for optimising preparation parameters for removal of each dye.

A 3 level 3 factor Box Behnken (BBD) was performed using the software Design Expert 09.01.03 (Stat-Ease Inc. Minneapolis, USA) to find the interactive effects of the 3 factors, A (Temperature; °C), B (Time; min), C (Impregnation ratio). It is shown in (Table 1).

It requires only minimum number of experiments to be performed and also modeling is made possible by this method. In our case its only 17 runs for 3 factor 3 levels when Box Behnken method is used, instead of 27 runs using 2n factorial method.

## Results and Discussion

### Thermo gravimetric analysis of the raw date pits

TGA profile of date pits (Figure 3) shows two stages of weight loss. Weight loss from 57.79°C – 108.28°C showing 7.883 weight loss, can be attributed to the removal of moisture and volatile contents. The major weight loss of 46.02% observed from 283.79°C – 319.99°C shows the decomposition of hemicelluloses, cellulose and lignin. The decomposition temperatures of these fractions depend on the lignocellulosic material [23,24]. The decomposition temperature is found to be around 303.04°C which is in match with the literature value. At temperatures above 350°C, significant weight loss was not observed. Therefore, it can be stated that the temperatures above 350°C is more appropriate for activation.

### Chemical activation

Date pits source was chemically activated. As the preparation conditions vary, the surface properties and the pore structure of the prepared activated carbon will vary accordingly [25]. Hence the molecule which it can absorb varies with the preparation parameters. As already mentioned RSM was used to optimise the preparation parameters for the AC to effectively remove MB, MG, MV and MR dye and molecules of size < 2nm from the aqueous solution.

**Development of regression model:** As already mentioned, Box Behnken design [26,27] was used to develop a correlation between the preparation process variables and the responses - yield, iodine number (I No.), methyl red (MR No.), methylene blue (MB No.), malachite green number (MG No.) and methyl violet number (MV No.). If our aim is to prepare AC that has to separate out MB dye, then optimisation is done having yield and methylene blue number

**Table 2:** Analysis of variance (ANOVA) for response surface quadratic model for activated carbon yield.

ANOVA for Response Surface Reduced Quadratic model						
Analysis of variance table [Partial sum of squares - Type III]						
	Sum of		Mean	F	p-value	
Source	Squares	df	Square	Value	Prob > F	
Model	14015.12	7	2002.16	195.52	< 0.0001	significant
A-temperature	6500.34	1	6500.34	634.79	< 0.0001	
B-time	3938.24	1	3938.24	384.59	< 0.0001	
C-impregnation ratio	1902.83	1	1902.83	185.82	< 0.0001	
AB	965.31	1	965.31	94.27	< 0.0001	
AC	299.12	1	299.12	29.21	0.0004	
BC	369.6	1	369.6	36.09	0.0002	
C^2	39.68	1	39.68	3.88	0.0805	
Residual	92.16	9	10.24			
Lack of Fit	91	5	18.2	62.73	0.0007	significant
Pure Error	1.16	4	0.29			
Corrected Total	14107.28	16				

**Table 3:** Analysis of variance (ANOVA) for response surface quadratic model for Iodine Number.

ANOVA for Response Surface Reduced Quadratic model						
Analysis of variance table [Partial sum of squares - Type III]						
	Sum of		Mean	F	p-value	
Source	Squares	df	Square	Value	Prob > F	
Model	13653.43	9	1517.05	115.31	< 0.0001	significant
A-temperature	5799.32	1	5799.32	440.81	< 0.0001	
B-time	4519.44	1	4519.44	343.53	< 0.0001	
C-impregnation ratio	1902.83	1	1902.83	144.64	< 0.0001	
A^2	64.68	1	64.68	4.92	0.0261	
B^2	1.32	1	1.32	0.1	0.034	
Residual	92.09	7	13.16			
Lack of Fit	90.93	3	3.31	14.46	0.0703	not significant
Pure Error	1.16	4	0.29			
Corrected Total	13745.52	16				

as response. Similarly for removing molecules of size < 2nm, the yield and iodine number were considered as the response. The optimisation part was done for all the adsorbents considered corresponding to the raw source.

The experimental data were analyzed using Design Expert. Three main analytical steps are

1. Analysis of variance (ANOVA)
2. Regression analysis
3. Plotting of response surface.

They were performed to establish an optimal condition for the activated carbon preparation. The highest order polynomials were chosen based on the sequential model sum of squares. The analysis

**Table 4:** Analysis of variance (ANOVA) for response surface quadratic model for Methyl Red Number.

ANOVA for Response Surface Reduced Quadratic model						
Analysis of variance table [Partial sum of squares - Type III]						
	Sum of		Mean	F	p-value	
Source	Squares	df	Square	Value	Prob > F	
Model	362.21	9	40.25	15.63	0.0008	significant
A-temperature	32.4	1	32.4	12.59	0.0094	
B-time	47.06	1	47.06	18.28	0.0037	
C-impregnation ratio	99.67	1	99.67	38.72	0.0004	
AC	0.16	1	0.16	0.064	0.008	
BC	17.78	1	17.78	6.91	0.034	
A^2	36.99	1	36.99	14.37	0.0068	
Residual	18.02	7	2.57			
Lack of Fit	14.43	3	4.81	5.36	0.0693	not significant
Pure Error	3.59	4	0.9			
Corrected Total	380.23	16				

**Table 5:** Analysis of variance (ANOVA) for response surface quadratic model for Methylene Blue Number.

ANOVA for Response Surface Reduced Quadratic model						
Analysis of variance table [Partial sum of squares - Type III]						
	Sum of		Mean	F	p-value	
Source	Squares	df	Square	Value	Prob > F	
Model	5751.87	7	821.7	57.76	< 0.0001	significant
A-Temperature	30.3	1	30.3	2.13	0.1785	
B-Time	178.3	1	178.3	12.53	0.0063	
C-Impregnation ratio	124.49	1	124.49	8.75	0.016	
AC	53.3	1	53.3	3.75	0.0849	
A^2	1629.63	1	1629.63	114.55	< 0.0001	
B^2	1190.54	1	1190.54	83.69	< 0.0001	
C^2	1988.23	1	1988.23	139.76	< 0.0001	
Residual	128.03	9	14.23			
Lack of Fit	112.47	5	22.49	5.78	0.057	not significant
Pure Error	15.56	4	3.89			
Corrected Total	5879.91	16				

suggested a quadratic model for all the responses except for methyl violet number for date pits source which fitted 2FI model. The model and factor significances were investigated using the variance analysis (ANOVA) from the F test and p-values at 95% confidence. If the value of Prob > F is less than 0.05, the model terms are considered as significant. In case if the terms are insignificant these terms can be removed from the model equation in order to increase the R<sup>2</sup> value, so as to improve the fitting. After the insignificant terms are removed, these are the final experimental model obtained for each of the response. The responses yield, iodine number, methyl red number, methylene blue number, malachite green number and methyl violet number are named Y<sub>1</sub>, Y<sub>2</sub>, Y<sub>3</sub>, Y<sub>4</sub>, Y<sub>5</sub> and Y<sub>6</sub>. The final experimental models in terms of coded factors for the responses are as follows:



**Table 6:** Analysis of variance (ANOVA) for response surface quadratic model for Malachite Green Number.

ANOVA for Response Surface Reduced Quadratic model						
Analysis of variance table [Partial sum of squares - Type III]						
	Sum of		Mean	F	p-value	
Source	Squares	df	Square	Value	Prob > F	
Model	14015.12	7	2002.16	195.52	< 0.0001	significant
A-Temperature	6500.34	1	6500.34	634.79	< 0.0001	
B-Time	3938.24	1	3938.24	384.59	< 0.0001	
C-Impregnation ratio	1902.83	1	1902.83	185.82	< 0.0001	
AB	965.31	1	965.31	94.27	< 0.0001	
AC	299.12	1	299.12	29.21	0.0004	
BC	369.6	1	369.6	36.09	0.0002	
C <sup>2</sup>	39.68	1	39.68	3.88	0.0805	
Residual	92.16	9	10.24			
Lack of Fit	91	5	18.2	62.73	0.0007	significant
Pure Error	1.16	4	0.29			
Corrected Total	14107.28	16				

**Table 7:** Analysis of variance (ANOVA) for response surface quadratic model for Methyl Violet Number.

ANOVA for Response Surface Reduced Quadratic model						
Analysis of variance table [Partial sum of squares - Type III]						
	Sum of		Mean	F	p-value	
Source	Squares	df	Square	Value	Prob > F	
Model	13395.73	6	2232.62	210.14	< 0.0001	significant
A-Temperature	4962.07	1	4962.07	467.05	< 0.0001	
B-Time	3598.91	1	3598.91	338.74	< 0.0001	
C-Impregnation ratio	1893.59	1	1893.59	178.23	< 0.0001	
AB	1456.95	1	1456.95	137.13	< 0.0001	
AC	1092.96	1	1092.96	102.87	< 0.0001	
BC	391.25	1	391.25	36.83	0.0001	
Residual	106.24	10	10.62			
Lack of Fit	94.08	6	15.68	5.15	0.0672	not significant
Pure Error	12.17	4	3.04			
Corrected Total	13501.97	16				

$$Y_1 = + 53.00 - 4.80A - 5.00B - 1.91C + 1.67AB + 1.458A^2 - 1.17C^2 \quad (6)$$

$$Y_2 = + 979.40 + 25.51A + 15.30B + 6.16C - 32.60A^2 - 12.55B^2 \quad (7)$$

$$Y_3 = + 209.68 + 6.03A + 3.92B + 0.53C - 3.25AC - 1.74BC - 5.32A^2 \quad (8)$$

$$Y_4 = + 215.58 - 1.95A + 4.72B + 3.94C + 3.65AC - 19.520A^2 - 16.66B^2 - 21.57C^2 \quad (9)$$

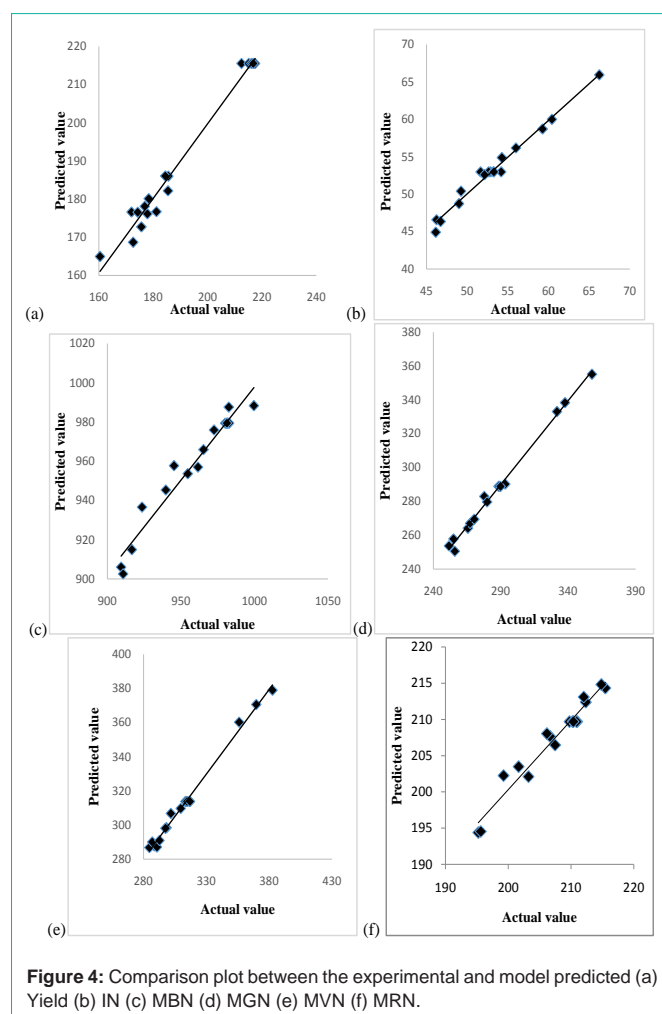
$$Y_5 = + 288.8 + 28.51A + 22.19B + 15.42C + 15.53AB + 8.65AC + 9.61BC - 3.06C^2 \quad (10)$$

$$Y_6 = + 313.76 + 34.91A + 21.21B + 15.38C + 19.08AB + 16.53AC + 9.89BC \quad (11)$$

Negative sign in the above equations indicate antagonistic effect, whereas positive sign indicates synergistic effect. The proximity of R<sup>2</sup> value to unity, indicate the suitability of the model equation. The R<sup>2</sup> values of all the responses are relatively high, indicating good agreement between experimental data and the model prediction.

The ANOVA of the models chosen corresponding to the responses Y<sub>1</sub>, Y<sub>2</sub>, Y<sub>3</sub>, Y<sub>4</sub>, Y<sub>5</sub> and Y<sub>6</sub> are given in (Table 2-7). ANOVA is mainly involved to examine the quality of the proposed model. From the ANOVA table, for activated carbon yield (Table 2), an F-value of 195.52 and Prob > F of less than 0.0001 prove the significance of the model. Also the model terms A, B and C and their interaction terms shown in Table had Prob > F values less than 0.05 indicating that all are significant. Also the higher values of R<sup>2</sup> (0.92) and R<sup>2</sup>adj (0.944) confirms that the postulated model is suitable to be used within the range of factors analyzed.

Similarly, the ANOVA tables obtained for the rest of the responses (Table 3-7) F values were found to be 115.31, 15.63, 57.76, 195.52, 210.14 and Prob > F were also less than 0.0001. These statistical test results show the validity of the chosen model. The predicted yield and adsorption capacity values from the above equations are given in (Table 8, Figure 4) shows the comparison between the adsorption capacities obtained through experiments and that predicted by

**Figure 4:** Comparison plot between the experimental and model predicted (a) Yield (b) IN (c) MBN (d) MGN (e) MVN (f) MRN.

**Table 8:** Actual and model predicted values of yield, IN, MRN, MBN, MGN and MVN by Box Behnken design.

Run order	(A)	(B)	(C)	Yield		IN		MRN		MBN		MGN		MVN	
				Actual value	Predicted value	Actual value	Predicted value	Actual value	Predicted value	Actual value	Predicted value	Actual value	Predicted value	Actual value	Predicted value
1	400	60	2	59.57	58.52	980.1	979.4	210.3	209.68	212.47	215.58	288.56	288.89	314.56	313.76
2	400	60	2	58.92	58.52	981.8	979.4	210.8	209.68	215.12	215.58	288.57	288.89	313.21	313.76
3	350	30	2	56.76	57.18	909.2	905.99	195.2	194.4	172	176.63	251.53	253.74	284.65	286.73
4	400	60	2	58.07	58.52	981.2	979.4	210.9	209.68	216.08	215.58	288.62	288.89	314.59	313.76
5	350	60	1	55.86	53.67	910.6	902.58	195.6	194.55	177.89	176.14	255.86	250.55	286.85	290
6	400	60	2	57.83	58.52	982.7	979.4	209.7	209.68	216.76	215.58	288.49	288.89	316.85	313.76
7	400	90	3	43.65	43.51	999.5	988.3	212.3	212.39	185.56	186.01	331.56	333.05	356	360.25
8	400	30	1	55.39	56.68	939.6	945.39	201.6	203.48	172.65	168.68	254.85	257.84	290.56	287.06
9	450	30	2	51.78	52.03	961.5	957.01	207.4	206.47	175.68	172.74	279.79	279.68	298.25	298.37
10	450	60	3	40.25	40.33	965.3	965.92	206.6	207.68	178.39	180.14	337.58	338.41	369.56	370.58
11	400	60	2	58.21	58.52	981.2	979.4	210.2	209.68	217.46	215.58	288.76	288.89	316.5	313.76
12	450	90	2	40.86	40.44	982.5	987.61	215.4	214.32	185.47	182.18	357.56	355.12	382.5	378.96
13	450	60	1	45.12	45.21	954.6	953.61	212	213.11	160.47	164.95	293.26	290.27	301.64	306.75
14	350	90	2	52.45	52.2	923.5	936.59	199.2	202.25	184.47	186.07	267.17	267.04	292.56	290.98
15	400	90	1	47.59	48.4	972.5	975.99	214.8	214.82	176.89	178.12	277.67	282.98	309.54	309.7
16	350	60	3	46.76	48.78	916.5	914.89	203.2	202.1	181.21	176.73	265.59	264.1	288.65	287.71
17	400	30	3	53.76	51.8	945.2	957.7	206.1	208.03	174.29	176.57	270.29	269.46	297.46	298.05

Eq. (6) to (11). The final model can be used to create graphical representations of the parameter dependencies, e.g., as contour plots, to see the relative influence of the parameters and to find an optimum parameter combination. The predicted values got from RSM model were then compared with the actual values to examine if they are close enough to test the compatibility of the model.

#### Interaction effects of the preparation parameters on the yield:

The yield and adsorption capacities of the prepared activated carbon (ACDP) over different combinations of independent variables were visualized through three-dimensional view of response surface plots (Figure 5 (a), (b) and 6 (a) to 5 (h)). The plots were represented as a function of two factors at a time, holding other factors at a fixed level.

Effect of AC preparation variables on the AC yield is shown in the (Figure 5 (a) and (b) which represent the effect of activation temperature and time on the yield, with impregnation ratio fixed at zero level (i.e., IR = 2) and the effect of time and impregnation ratio

on the yield, with temperature fixed at zero level (i.e., T = 400°C). The carbon yield was found to decrease with increasing activation temperature, activation time and IR. From the (Figure 5(a)), as the time and temperature was increased from 30 min to 90 min and 350°C to 450°C respectively, yield decreased. From both figures, it can be seen that activation temperature was more influential than the other two variables. However, the maximum yield was observed when all these factors were set to the minimum value in the range studied. This result was found to be in agreement with the work done by Ahmad et al. and Islay et al., [2,23] which found that activation temperature plays a crucial role on the yield of activated carbon prepared by rattan sawdust and grape stalk whereas activation time did not show much effect on the carbon yield. Overall weight loss was found to increase with increasing temperature, resulting in decreasing yield of activated carbon at high temperature. As a result of removal of volatile matters during the dehydration and elimination reactions and increased rate of CO<sub>2</sub> formation reaction, the overall weight loss was found to increase with increasing temperature thus lowering the yield. Coming to impregnation ratio, (Figure 5(b)) shows that increased impregnation ratio results in increased carbon burn-off and decreased yield. This can be attributed to the increased breakage of carbon bonds with increased amount of oxidising agent thus promoting more of coal decomposition during pyrolysis.

Referring to (Table 3), all the three factors were found to be significantly influencing the response for activated carbon yield, with activation temperature imposing the greatest effect on it, while the other two showed almost similar and moderate effect on this response. However, the interaction effects between the variables were all less significant. Similarly, (Figure 5(a) and (b)) shows the influence of time on the yield, indicating that the increased activation time causes decrease in yield as well.

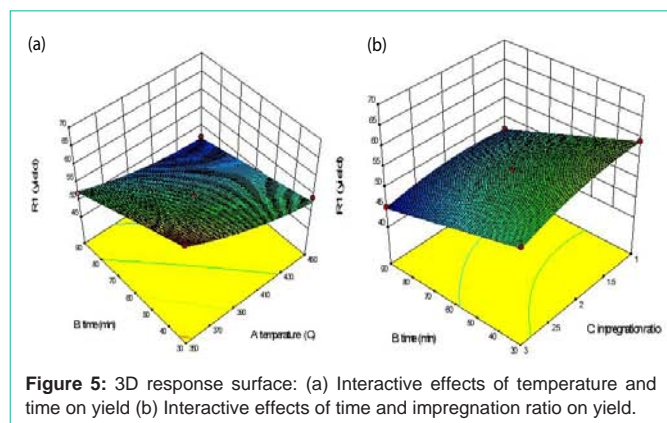


**Figure 5:** 3D response surface: (a) Interactive effects of temperature and time on yield (b) Interactive effects of time and impregnation ratio on yield.

**Interaction effects of the preparation parameters on the adsorption characteristics: MB / MG / MV / MR number:** The effect of various preparation parameters on the adsorption characteristics of the prepared AC was investigated and the results are shown in (Figure 6(a) to (h)). It was observed that the pore size and hence the surface area of the samples significantly increased with raise in the activation temperature holding the other factors constant. Similar results were observed when the activation time and impregnation ratio was increased maintaining the other factors constant. It can be well said that most of the organic substances have got degraded and discharged both as gas and liquid tars hence leaving high purity

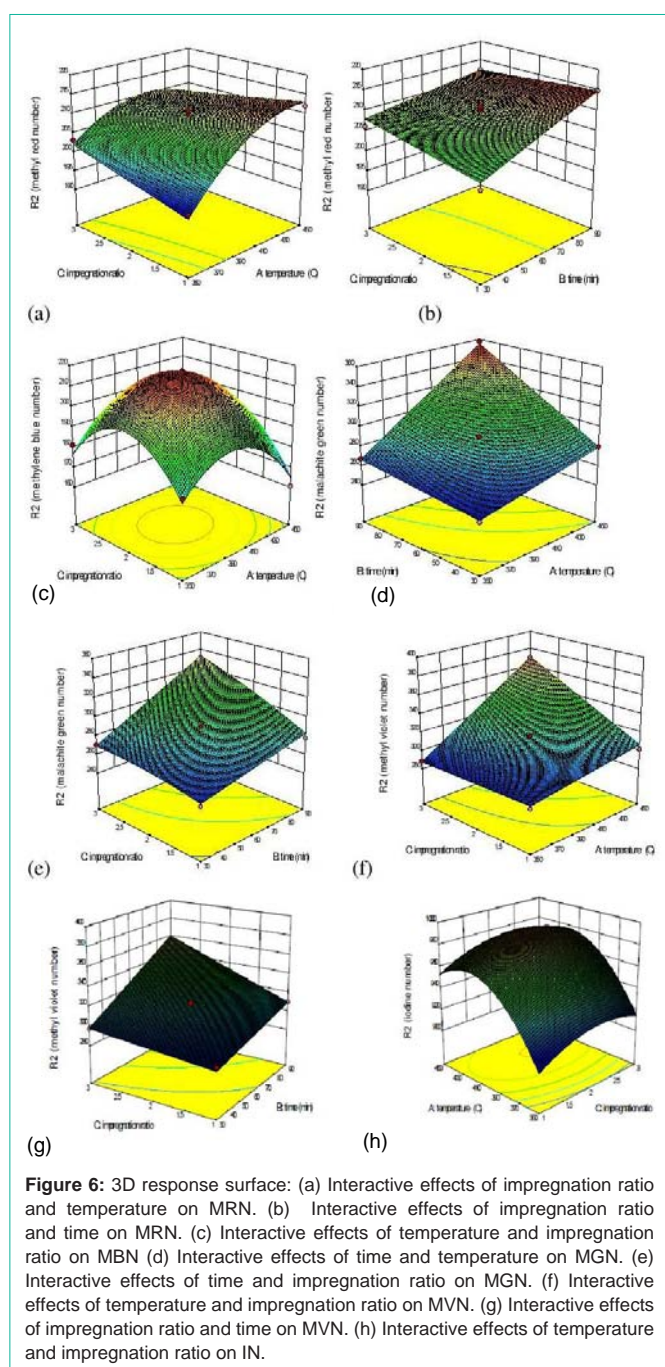


**Table 9:** Optimum preparation conditions for different molecular size.

Source	Adsorbate	Molecular weight (g/mol)	Activation temperature (°C)	Activation time (min)	Impregnation ratio
Date pits	IN	253.81	416.05	90	2.00687
	MR	269.3	360.67°C	33.95	2.474
	MB	319.85	370.284	48.29	1.93
	MG	364.91	420.117	52.78	2.03
	MV	407.98	449.37	68.991	2.959

**Table 10:** Comparison of predicted and experimental response values for the AC prepared at optimum conditions.

Adsorbate	Yield		Adsorptive capacity	
	Predicted	Experimental	Predicted	Experimental
IN	46.633	47.286	999.57	998.24
MR	62.3627	60.548	200.415	198.29
MB	59.102	57.989	205.174	204.648
MG	50.695	50.241	309.04	306.463
MV	43.44	45.175	383.619	380.214

carbon with high porosity at higher levels of these parameters. With this investigation of the influence of the factors, the next step of optimisation was carried out.

**Optimization of preparation parameters:** Optimization was carried out after observing all the interaction effects between the preparation variables [28]. A set of solutions were generated by the Design-Expert software, to determine the optimum conditions of the process. The optimization study was performed by considering the range of variables used in the experiment (i.e., activation temperature 350°C - 450°C; adsorption time 30-90 min; impregnation ratio 1-3) for the maximum response. Initially, the optimization was started at any random value of the individual variables by fixing the target of maximum adsorption capacity and obtaining the optimum values of the variables for the preparation process.

The experiment was conducted at the optimized conditions (Table 9) and a comparison between the experimental values and model predicted results was found to be good, as in (Table 10).

**Scanning electron microscopy (SEM)**

Scanning electron micrographs shown in (Figure 7) shows the surface morphology of the raw date pits source. SEM images are observed to be irregular clumps and not much pores were observed. The surface of the date pits is moderately smooth, has less cracks and voids than the activated carbon prepared.

SEM image of ACDP prepared at optimum conditions for MB removal is shown in the (Figure 8). The thick wall in the raw material opened and wider porosity was created by the activation. It can be confirmed that the activated carbon prepared has porous surface with cracks, channels, large holes and well pronounced array of structures. The surface morphology of the activated carbon samples prepared for the removal of other dyes is similar to that obtained for MB removal.

**Fourier transform infrared spectroscopy (FTIR)**

The surface chemistry of samples was analyzed through



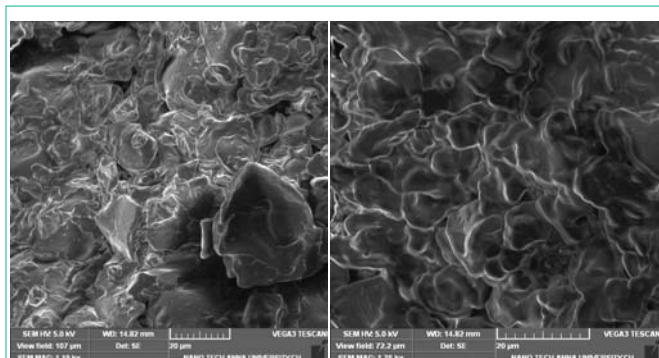


Figure 7: SEM image of raw date pits (RDP).

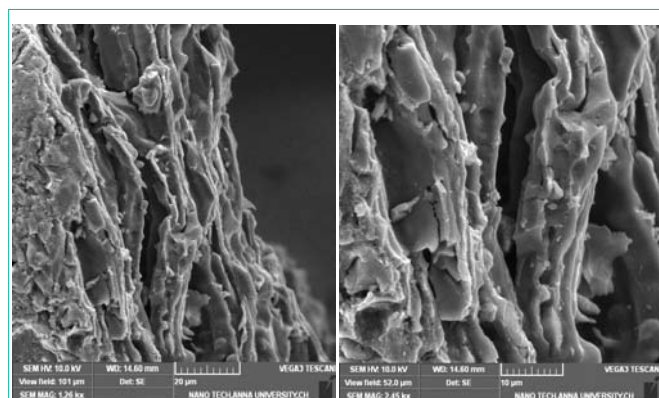


Figure 8: SEM image of ACDP prepared at optimum conditions for MB removal.

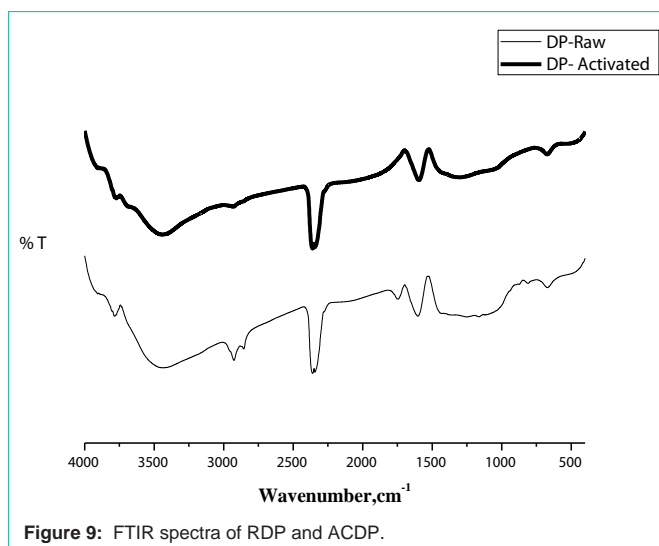


Figure 9: FTIR spectra of RDP and ACDP.

FTIR transmission spectra (Figure 9) recorded using a FTIR spectrophotometer in the wave number range of 4000 - 400  $\text{cm}^{-1}$ . In the FTIR spectrum obtained for the precursor, the band at about 3736 and 3432  $\text{cm}^{-1}$  was attributed to vibrations in hydroxyl groups. The vibrational peak at 2926 and 2855  $\text{cm}^{-1}$  can be due to the C-H stretching vibrations. The band located around 2344 and 2359  $\text{cm}^{-1}$  corresponds to atmospheric carbon dioxide. The peaks observed at 1751, 1602, 1252, 1165, 1115, 813, 670  $\text{cm}^{-1}$  are due to the C=O, C-C,

C-N, alkyl halides, =C-H bending vibration and N-H/alkene/alkyne stretching vibrations respectively.

Similar groups were found in the activated carbon sample prepared for MB removal when compared with RDP. Not much peaks were observed in the FTIR spectrum of ACDP which may be due to the hydrolysis effect of  $\text{H}_3\text{PO}_4$  resulting in the decomposition of these groups and subsequent release of their byproducts as volatile matter. The surface functional groups of the other activated carbon samples were also analysed and the peaks obtained are similar to that of ACDP for MB removal.

## Conclusion

Date pits, a waste biomass can be picked to be a better precursor for preparing activated carbon by chemical activation with phosphoric acid. As the preparation parameters were found to directly influence the surface properties, the activated carbon can be tailor-made to suit the need. The activation process was confirmed by the well developed pore structure seen in SEM image and the FTIR analysis. The significant effect of three important process parameters were investigated systematically and optimised preparation condition was determined for the prepared ACDP to separate out different dyes of varying molecular weight range using RSM. This work showed that the effectiveness of an adsorbent lies in the way it is prepared and tuning the preparation condition directly has effect on the pore structure. Hence depending upon the size of the molecule we can use the particular preparation condition which is generalised for that molecular size range for a specific source.

## References

1. Nomanbhay S and Palanisamy K. Removal of heavy metal from industrial 426 waste water using chitosan coated oil palm shell charcoal, *Electronic Journal of Biotechnology*. 2005; 8: 43–53.
2. Ahmad AA, Hameed BH, Aziz N. Adsorption of direct dye on palm ash: kinetic and equilibrium modeling. *J Hazard Mater*. 2007; 141: 70-76.
3. Hameed BH, Ahmad AA and Aziz N. Isotherms, kinetics and thermodynamics of acid dye adsorption on activated palm ash, *Chemical Engineering Journal*, 2007; 133: 195–203.
4. Hasan M, Ahmad AL and Hameed BH. Adsorption of reactive dye onto cross-linked chitosan/oil palm ash composite beads, *Chemical Engineering Journal*, 2008; 136: 164–172.
5. Hameed BH, Mahmoud DK and Ahmad AL. Sorption of basic dye from aqueous solution by pomelo (*Citrus grandis*) peel in a batch system, *Colloids Surf. A: Physico chem. Eng. Aspects*, 2008; 316: 78–84.
6. Batzias FA, Sidiras DK. Simulation of methylene blue adsorption by salts-treated beech sawdust in batch and fixed-bed systems. *J Hazard Mater*. 2007; 149: 8-17.
7. Mittal A, Malviya A, Kaur D, Mittal J, Kurup L. Studies on the adsorption kinetics and isotherms for the removal and recovery of Methyl Orange from wastewaters using waste materials. *J Hazard Mater*. 2007; 148: 229-240.
8. Demir H, Top A, Balköse D, Ulkü S. Dye adsorption behavior of Luffa cylindrica fibers. *J Hazard Mater*. 2008; 153: 389-394.
9. Osma JF, Saravia V, Toca-Herrera JL, Couto SR. Sunflower seed shells: a novel and effective low-cost adsorbent for the removal of the diazo dye Reactive Black 5 from aqueous solutions. *J Hazard Mater*. 2007; 147: 900-905.
10. Vilar VJP, Botelho CMS and Boaventura RAR. Methylene blue adsorption by algal biomass based materials: biosorbents characterization and process behaviour, *Journal of Hazardous materials*, 2007; 147: 120–132.



11. Çiçek F, Ozer D, Ozer A, Ozer A. Low cost removal of reactive dyes using wheat bran. *J Hazard Mater.* 2007; 146: 408-416.
12. Ponnusami V, Vikram S, Srivastava SN. Guava (*Psidium guajava*) leaf powder: novel adsorbent for removal of methylene blue from aqueous solutions. *J Hazard Mater.* 2008; 152: 276-286.
13. Doulati Ardejani F, Badii Kh, Limaee NY, Shafaei SZ, Mirhabibi AR. Adsorption of Direct Red 80 dye from aqueous solution onto almond shells: effect of pH, initial concentration and shell type. *J Hazard Mater.* 2008; 151: 730-737.
14. Ozer D, Dursun G, Ozer A. Methylene blue adsorption from aqueous solution by dehydrated peanut hull. *J Hazard Mater.* 2007; 144: 171-179.
15. Kalavathy MH, Karthikeyan T, Rajgopal S, Miranda LR. Kinetic and isotherm studies of Cu(II) adsorption onto H<sub>3</sub>PO<sub>4</sub>-activated rubber wood sawdust. *J Colloid Interface Sci.* 2005; 292: 354-362.
16. Helen Kalavathy M. and Lima Rose Miranda, *Moringa oleifera* - A solid phase extractant for the removal of copper, nickel and zinc from aqueous solutions, *Chemical Engg Journal*, 2010; 158: 188 – 199.
17. Padmini E, Helen Kalavathy M and Lima Rose Miranda. Surface modified *Agave sisalana* as an adsorbent for the removal of nickel from aqueous solutions – Kinetic and Equilibrium studies, *Carbon letters*, 2008; 9: 97-104.
18. Bulut Y, Gözübenli N, Aydın H. Equilibrium and kinetics studies for adsorption of direct blue 71 from aqueous solution by wheat shells. *J Hazard Mater.* 2007; 144: 300-306.
19. ASTM, Standard test method for determination of iodine number of activated carbon, D 4607-94, 2006; 1-5.
20. BIS, Determination of decolorizing power, IS: 877-1977; 9-10.
21. Niya AA, Daud WMAW, Mjalli FS, Abnisa F and Shafeeyan MS. Production of microporous palm shell based activated carbon for methane adsorption: Modeling and optimization using response surface methodology, *Chemical Engineering Research and Design*, 2012; 90: 776–784.
22. Gratuito MKB, Panyathanmaporn T, Chumnanklang RA, Sirinunta wittaya N and Dutta A. Production of activated carbon from coconut shell: Optimization using response surface methodology, *Bioresource Technology*, 2008; 99: 4887–4895.
23. Ozdemir I, Sahin M, Orhan R and Erdema M. Preparation and characterization of activated carbon from grape stalk by zinc chloride activation, *Fuel Processing Technology*, 2014; 125: 200–206.
24. Saka C. BET, TG–DTG, FT-IR, SEM, iodine number analysis and preparation of activated carbon from acorn shell by chemical activation with ZnCl<sub>2</sub>, *Journal of Analytical and Applied Pyrolysis*. 2012; 95: 21–24.
25. Mall ID, Srivastava VC, Kumar GVA, Mishra IM. Characterization and utilization of mesoporous fertilizer plant waste carbon for adsorptive removal of dyes from aqueous solution, *Journal of Colloids and Surfaces: Physicochem. Eng. Aspects*, 2006; 278: 175-187.
26. Chen YD, Chen WQ, Huang B and Huan MJ. Process optimization of K<sub>2</sub>C<sub>2</sub>O<sub>4</sub>-activated carbon from kenaf core using Box–Behnken design, *Chemical Engineering Research and Design*, 2013; 91: 1783–1789.
27. Das D, Vimala R and Das N. Biosorption of Zn(II) onto *Pleurotus platypus*: 5-Level Box–Behnken design, equilibrium, kinetic and regeneration studies, *Ecological Engineering* 2014; 64: 136–141.
28. Ahmad MA and Alrozi R, Optimization of preparation conditions for mangosteen peel-based activated carbons for the removal of Remazol Brilliant Blue R using response surface methodology, *Chemical Engineering Journal*, 2010; 165: 883–890.